

¹ Atmospheric Science Laboratory, Department of Geography, East Carolina University, NC, USA

² Department of Geography and Geology, UNC Wilmington, NC, USA

Regional variations of the Caribbean mid-summer drought

S. Curtis¹, D. W. Gamble²

With 8 Figures

Received 2 April 2007; Accepted 4 July 2007; Published online 9 November 2007

© Springer-Verlag 2007

Summary

Pentad satellite-based precipitation estimates were input into a wavelet analysis to quantify the length, timing, and strength of the mid-summer drought (MSD) for the Caribbean Sea and surrounding regions. For most of the Caribbean the time between the first and second summer precipitation maxima is 98 to 117 days (~3 to 4 months). The MSD appears in early-June over Puerto Rico and Hispaniola, and develops progressively later in the summer season towards the west, finally occurring in early-October over the Gulf of Mexico. The MSD is most intense in the eastern Pacific, strong and significant in the western Caribbean, and almost nonexistent in the eastern Caribbean. Forcing mechanisms are examined to help explain the regional variability in the Caribbean. A July increase in surface pressure and surface divergence, caused by the changing wind field, appears to contribute to a strong concurrent MSD over the waters bounded by Jamaica, Cuba, and the Yucatan peninsula. Finally, the island of Jamaica itself appears to block the flow of the tradewinds as they migrate northward and intensify into mid-summer, thus enhancing the divergence, and in turn MSD, immediately to the west.

1. Introduction

The precipitation climatology of certain regions of the northern hemisphere tropics can be char-

acterized by a bimodal summertime rainy season. Sometimes this bimodality is explained by a double-peak in the latitude position of the Inter-tropical Convergence Zone (ITCZ). One such example occurs in Nigeria and western Africa, which experience a “little dry season” (Adejuwon and Odekunle 2006). Southern Mexico and Central America also experience a severe mid-summer drought (MSD), which can be up to a 40% reduction of rainfall from one month to the next during the summer season (Hastenrath 1967). Hastenrath (2002) also regards the position of the ITCZ as a major factor in producing the MSD in this region of the tropics. However, Magaña et al. (1999) contend that the MSD in southern Mexico and Central America is caused by local air-sea interactions, namely a build up of convective clouds in the early summer season leading to a shadowing effect and cooling of the eastern Pacific, followed by anomalous anti-cyclonic circulation and divergence of low level winds. The nearby Caribbean Sea also experiences a MSD, although not as strong as the eastern Pacific (Curtis 2002). Interestingly, the MSD in the Caribbean appears to be generated by different mechanisms as compared to the eastern Pacific. Giannini et al. (2000) propose that an intensification and expansion of the North Atlantic Subtropical High (NASH) during mid-

Correspondence: Dr. Scott Curtis, Assistant Professor, Atmospheric Science Laboratory, Department of Geography, East Carolina University, Brewster A232, Greenville, NC 27858, USA, e-mail: CURTISW@ecu.edu

summer is responsible for overall subsidence and less rainfall.

The variability of the timing and severity of northern hemisphere bimodal rainy seasons has significant implications for rain-fed agriculture and water management. The Nigerian MSD extends between mid- to late-July and late-August to early-September, and the variability is largely controlled by sea surface temperature (SST) anomalies in the Gulf of Guinea (Adejuwon and Odekunle 2006). The eastern Pacific MSD is centered between late-July and early-August (Hastenrath 1967; Magaña et al. 1999) and varies interannually with the El Niño/Southern Oscillation (ENSO) cycle (Curtis 2002), with El Niños (La Niñas) associated with a strong (weak) MSD. Chen and Taylor (2002) noted a bimodal rainy season for the Caribbean as a whole, with the MSD occurring in July. Using this information, Angeles et al. (2007) created a bimodal index from the angles created by two vectors originating with the monthly rainfall total in July and ending with the monthly total in June (vector A) and August (vector B). They found that the strength of this index, and thus the MSD, was significantly related to vertical wind shear and Saharan dust concentration. However, Gamble et al. (2007) found the timing of the MSD varies substantially across the Caribbean islands. Rather than fixing the MSD to July, for the period from March to October they subtracted adjacent months and divided the result by the current month to create a time series of proportional differences. These values were then input into a principal component analysis (PCA). Gamble et al. (2007) identified six regions which had similar factor loadings in the PCA, with four consisting of multiple stations. For the *Eastern Rim* of the Caribbean the drought is centered on May–June, in the *Interior* (Hispaniola, Puerto Rico) the drought is prolonged into June–July, in the *Northwest Caribbean* (western Cuba and southern Florida) the drought is centered on July, and in the *Transition* zone (Jamaica and eastern Cuba) the drought is in July as well, but stronger than the *Northwest Caribbean* MSD. The westward shift in the timing of the MSD is consistent with Giannini et al.’s (2000) hypothesis of the westward expansion of the NASH. The PCA results have advanced our understanding of the variability of the Caribbean MSD, but are limited

by the monthly scale of analysis. Furthermore, Gamble et al.’s (2007) analysis is confined to 20 gauging stations on the periphery of the Caribbean basin.

The purposes of this study are twofold. First, we want to refine the Gamble et al. (2007) analysis to the sub-monthly scale and extend the spatial coverage to include the Caribbean Sea with satellite precipitation data. Second, we want to verify the westward migration of the MSD and make note of any other regional variations within the basin. While the literature suggests that the Caribbean MSD is forced on the large scale by the NASH, local air–sea–land interactions may play an important role in the timing and severity of the MSD, as is the case in the eastern Pacific (Magaña et al. 1999).

2. Data and methods

Precipitation in the Caribbean region (97.5° W to 60.0° W; 7.5° N to 27.5° N) estimated from multiple satellites and gauges, and averaged every 5 days (pentad) was obtained from the Global Precipitation Climatology Project (GPCP, Xie et al. 2003). An annual climatology for every 2.5° grid block in the domain was calculated from 1979 to 2005. An interactive data language (IDL) wavelet analysis (Torrence and Compo 1998) was chosen to describe the MSD. Wavelets are preferred over a fourier transform of the data (Curtis 2002) because the Caribbean MSD appears to be centered at different stages of the summer season (Gamble et al. 2007). Wavelets can identify the dominant modes of the MSD and the strength of these modes over the course of the annual cycle. A “time-average” significance test (Torrence and Compo 1998) was performed by comparing the global wavelet spectrum with the 99% level Monte Carlo runs of the time-averaged wavelet spectrum of white noise.

Before calculating the wavelet power spectrum, the annual mean precipitation was subtracted to create a time series of precipitation anomalies. Further, the anomaly time series was repeated three times to avoid edge effects in the wavelet analysis. The resulting power spectrum was only examined for wavelets with periods between 60-days (0.164 years) and 120-days (0.328 years). The former would approximate a June/August peak separated by a July minimum,

and the later represents a conservative temporal definition of the MSD, consistent with the March to October season defined in Gamble et al. (2007). Curtis (2002) examined the second order harmonic of global precipitation from May to October, which yields two peaks separated by 92-days (a 0.252-year periodicity). The wavelet analysis resolves four time scales within this defined range: 0.190-years, 0.226-years, 0.269-years, and 0.320-years. One of these four periods was recorded if there was a distinct peak in the wavelet power. The center of the MSD (temporally speaking) was defined as the pentad of maximum wavelet power for a given periodicity. This methodology was repeated for all 120 grid blocks in the Caribbean region. Results from the wavelet analysis were mapped in order to determine regional variations in the timing, duration, and magnitude of the MSD across the Caribbean.

Consistent with previous regional climate studies (Magaña et al. 1999; Giannini et al. 2000; Curtis 2004), geopotential height, vertical velocity (ω), and surface winds were examined to assess potential causes for Caribbean MSD

variability. The 30-year (1971–2000) pentad climatology of 1000 hPa and 500 hPa geopotential height and 700 hPa ω at 2.5° latitude-longitude resolution was obtained from the NCEP/NCAR reanalysis data set (Kalnay et al. 1996). This time period does not match the GPCP precipitation, but we assume that both data sets describe salient features of the long-term climatology, and are not greatly influenced by inter-annual variations, such as ENSO. QuikSCAT sea surface wind vectors produced by Remote Sensing Systems were obtained from 2000 to 2005 at 0.25° latitude-longitude resolution. Divergence was calculated at each grid block with the continuity equation, where Δu and Δv were taken from neighboring grid blocks to the east-west, and north-south, and Δx and Δy were 0.5° longitude and latitude, respectively.

3. Results

The results from the wavelet analysis for the GPCP grid block to the west of Jamaica (centered on 78.75° W; 18.75° N) are presented in

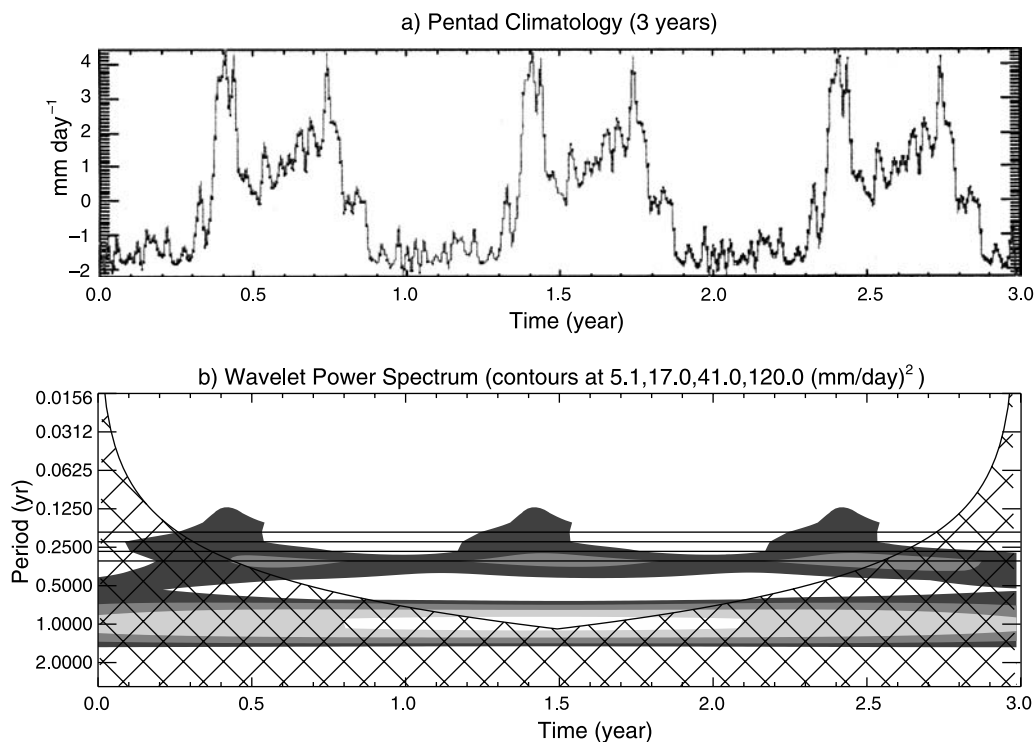


Fig. 1. Wavelet analysis of climatological GPCP pentad precipitation for the grid block centered at 78.75° W and 18.75° N. (a) annual precipitation anomaly time series repeated three times; (b) wavelet power spectrum. Contours of 5.1 (mm day^{-1})², 17.0 (mm day^{-1})², 41.0 (mm day^{-1})², and 120.0 (mm day^{-1})² are filled as dark grey, medium grey, light grey, and white, respectively. Horizontal lines denote 4 resolved MSD periods. Cross-hatched regions indicate the “cone of influence” where edge effects degrade the analysis

Fig. 1. Panel (a) is the anomalous precipitation climatology for years 1 to 3. There is an obvious mid-summer minimum at this location, with an onset of heavy precipitation in May, and a sudden decrease in precipitation around June 15 (0.45, 1.45, and 2.45 years). Subsequently, precipitation slowly recovers to a second maximum in late September. The shaded contours in the wavelet analysis (Fig. 1b) represent the power spectrum from 5.1 to 120.0 $[\text{mm day}^{-1}]^2$. The largest power is at the annual cycle, but there is a secondary maximum at the high end of the defined MSD range (horizontal lines on Fig. 1b). In summary, the MSD over the waters to the west of Jamaica peaks at the 0.320-year periodicity, with a maximum power value of 23.54 $[\text{mm day}^{-1}]$ on pentad July 5–9. Based on this analysis, the early wet period is defined as May 11 to June 14 and

an equal time interval of June 15 to July 19 is used to describe the core of the MSD.

Areas in the Caribbean domain where the wavelet analysis shows a distinct peak in periodicity between 60 and 120 days, and corresponding significances are mapped in Fig. 2. The majority of the grid blocks where the peak power falls outside the MSD range (92%) have a peak periodicity of 0.539-years (197 days), indicating two distinct rainy seasons separated by roughly six-months, rather than one bimodal rainy season. Nearly all of the MSDs in the region can be described with a periodicity of 0.269 (98 days) or 0.320-years (117 days), with the shorter MSD covering southern Mexico and Hispaniola, and the longer MSD stretching in a band from the eastern Pacific, through Cuba, and into the tropical Atlantic.

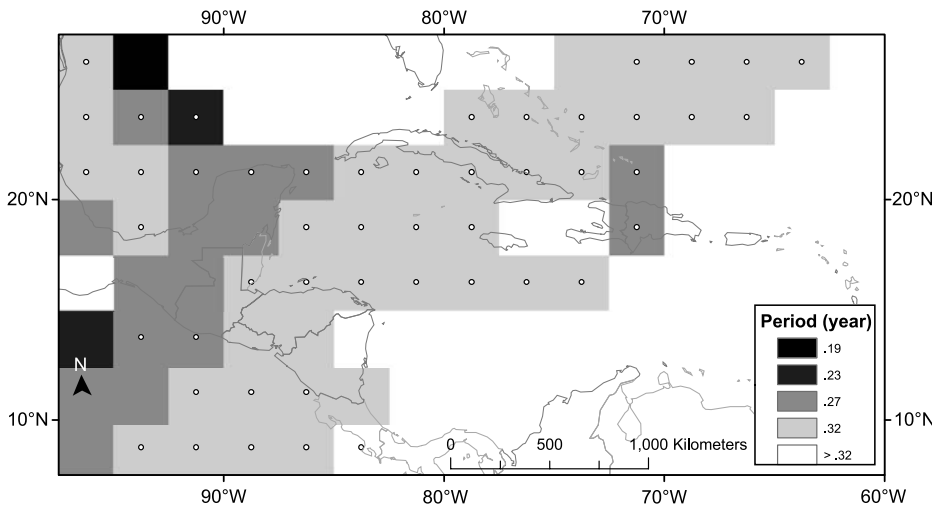


Fig. 2. Period (year) of maximum power in the wavelet spectrum between 0.164 (60 days) and 0.328 years (120 days). Circles denote 99% significant values determined by “time-average” test

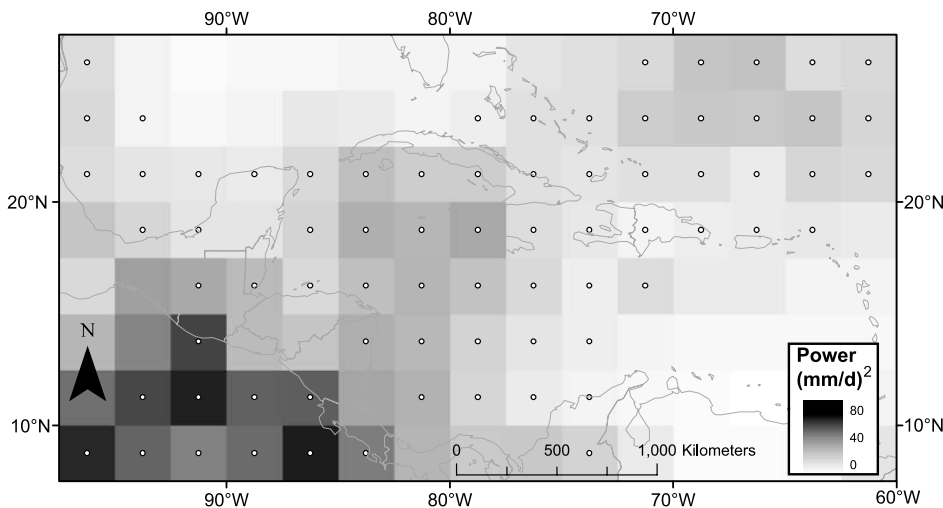


Fig. 3. Maximum power $(\text{mm day}^{-1})^2$ at the 0.320-year (117 day) period of the wavelet spectrum. Circles denote 99% significant values determined by “time-average” test

Regional variations of the Caribbean mid-summer drought

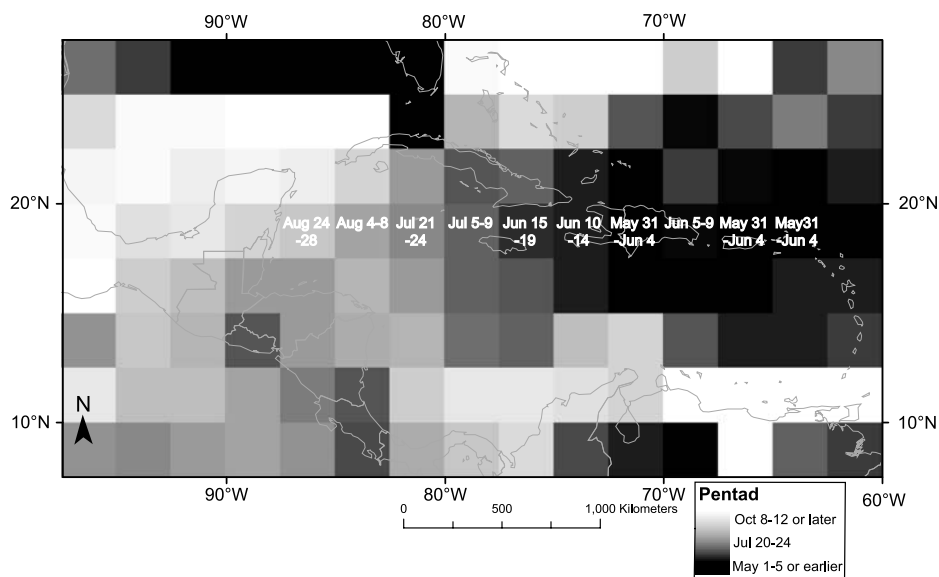


Fig. 4. Pentad of the maximum power displayed in Fig. 3. Blocks labeled along the 18.75° N parallel illustrate the progression of the MSD from east to west

Given that the 0.320-year (117 day) MSD dominates the eastern Pacific, Central America, and Caribbean, and is predominantly significant (38 out of 42 grid blocks), we choose to focus on this periodicity for the remainder of the paper. Figure 3 shows maximum wavelet power and significance at that time scale. The largest magnitudes (maximum 96.41 [mm day⁻¹]²) are situated in the eastern Pacific, consistent with Curtis (2002). However, significant values can be found in the western Gulf of Mexico, western Caribbean, and Atlantic. The part of the Caribbean that reaches significance roughly coincides with the *Interior*, *Transition*, and *Northwest Caribbean* regions of Gamble et al. (2007). The largest significant power value outside the eastern Pacific is the grid block to the west of Jamaica (Figs. 1 and 3). Figures 2 and 3 would suggest that the eastern Caribbean does not experience an MSD as defined here. Interestingly, much of Central America, southern Mexico, and western portion of the Pacific do not experience a *significant* MSD. From an examination of the wavelet plots, it appears that the annual cycle is dominating the global spectrum. Thus, while the MSD is recognized, the reduction in summertime rainfall is proportionally small.

Next, the pentad of the maximum power of the 0.320-year MSD is displayed in Fig. 4. Special attention should be given to the significant grid blocks from Fig. 3. The timing of the MSD in the eastern Pacific is fairly uniform, roughly falling between July 15 and August 23, consistent with

previous studies (Hastenrath 1967; Magaña et al. 1999). Figure 4 also confirms the westward movement of the MSD across the Caribbean (Gamble et al. 2007), with the MSD first appearing in early-June over Puerto Rico and Hispaniola (Fig. 4), and as late as early October in regions of the Gulf of Mexico (Fig. 4). The strongest “July-centered” MSD can be found in Jamaica and eastern Cuba (Fig. 4), consistent with the *Transition* grouping of Gamble et al. (2007).

The expansion of the NASH into the Caribbean may explain the MSD for the Caribbean as a whole, but reasons behind the discrepancy of the MSD between strong and significant in the western basin and weak to nonexistent in the eastern basin remain unclear. Thus, we examine local forcing mechanisms, namely geopotential height, vertical velocity, and surface winds, in regards to the relative maximum MSD to the west of Jamaica (Fig. 3). Particular attention is paid to the sudden onset that occurs around June 15 (Fig. 1). Figure 5 shows data for a grid block (centered at 80° W and 17.5° N), which overlaps the west Jamaica GPCP precipitation grid block. The geopotential height at 500 hPa is low in the winter and high in the summer (Fig. 5a), with the springtime transition occurring during the initial wet period. However, the time series is not bimodal. In the layer between 700 hPa (Fig. 5b) and 500 hPa air is rising, except in February–March–April. The dry season is marked by a sudden relaxation of the vertical velocity, but subsidence never occurs. This may be partly ex-

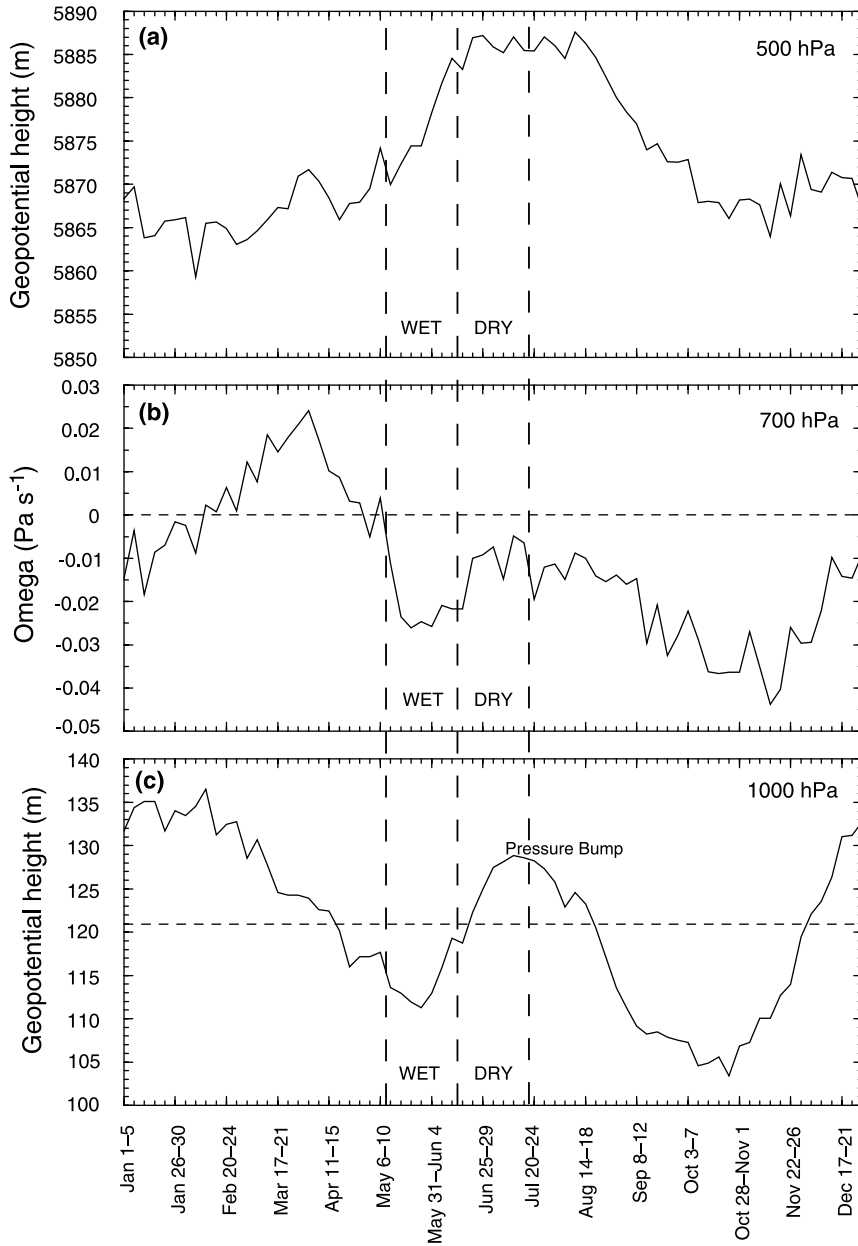


Fig. 5. Climatological NCEP/NCAR reanalysis data for the grid block centered at 80° W and 17.5° N. Early wet season and mid-summer dry season for that location are denoted. **(a)** Geopotential height (m) at 500 hPa, **(b)** vertical velocity in pressure coordinates (omega; Pa s^{-1}) at 700 hPa. Horizontal line marks zero. **(c)** Geopotential height (m) at 1000 hPa. Horizontal line is the annual average. Pressure bump discussed in the text is labeled

plained by the coarse data resolution and general difficulty in obtaining the omega field. During winter, the height of the 1000 hPa pressure surface is elevated (Fig. 5c) at the same time the 500 hPa surface is low (Fig. 5a). After a minimum in late May the near surface height begins to rise, reaching about 129 m on July 10–14, and then falls to a second minimum on October 23–27 (Fig. 5c). This pattern is roughly the inverse of the time series of precipitation (Fig. 1), where the wavelet analysis centers the MSD on July 5–9 (Fig. 4). In fact, the GPCP precipitation time series (Fig. 1) has a stronger correlation with

1000 hPa geopotential height (-0.58), than with 500 hPa geopotential height (0.55) or 700 hPa omega (-0.48).

Given the strong bimodality of the 1000 hPa geopotential height time series and fairly good inverse relationship with rainfall, we choose to investigate forcing mechanisms at the ocean surface. The first question to be addressed is whether the mid-summer pressure increase (“pressure bump”, Fig. 5c) controls the timing of the MSD across the Caribbean. A 1000 hPa height anomaly was calculated for each NCEP/NCAR grid block in the region by subtracting the annual mean

Regional variations of the Caribbean mid-summer drought

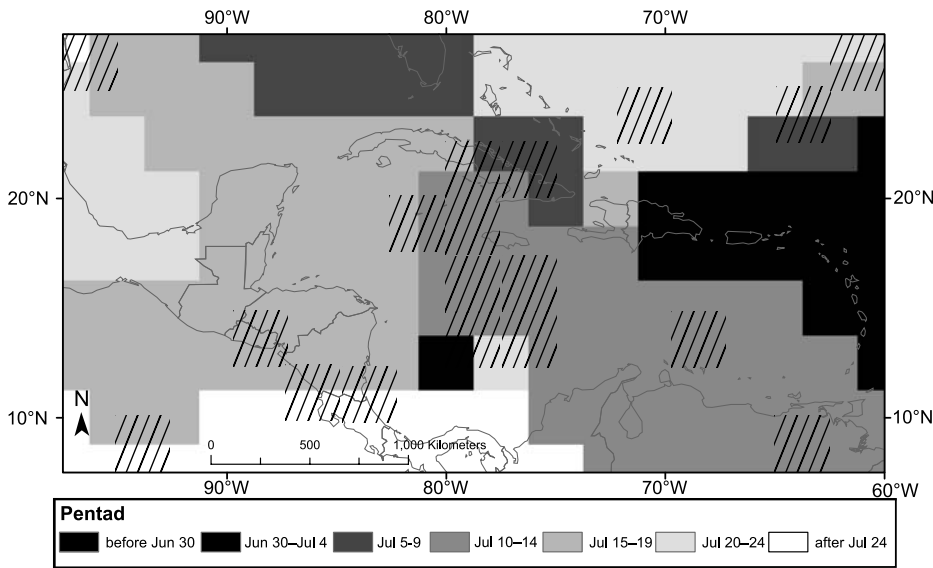


Fig. 6. Pentad of maximum climatological NCEP/NCAR 1000 hPa geopotential height between May 1–5 and October 8–12. Cross hatched areas show GPCP precipitation grid blocks where the pentad of maximum power (Fig. 4) occurred between June 30 and July 24

from the pentad observations. The pentad of the maximum height anomaly between May 1–5 and October 8–12 was then mapped on Fig. 6. This selection of dates is consistent with Fig. 4, and

avoids the winter pressure maximum. The relative maximum on July 10–14 (Fig. 5c) is clearly evident for all of Jamaica and much of the eastern Caribbean and northern South America

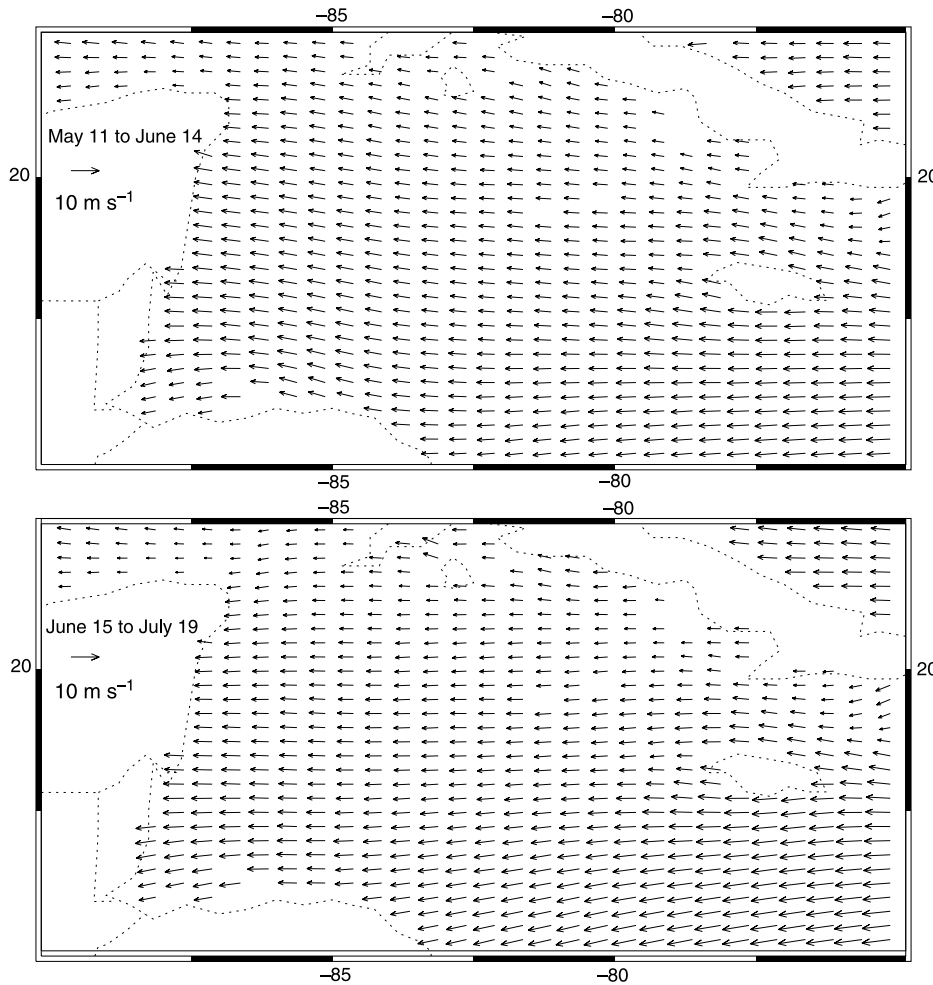


Fig. 7. Sea surface wind vectors for May 11 to June 14 (top panel) and June 15 to July 19 (bottom panel) averaged for the period 2000–2005

(Fig. 6). However, unlike the slow progression of the MSD across the Caribbean, there is an almost simultaneous increase in pressure. Figure 6 suggests a westward propagation in the maximum anomaly, but over the course of only 10 days (July 10–19). In fact, most of the domain experiences a maximum pressure anomaly between June 30 and July 24, which is consistent with the “July” model of the MSD in the Caribbean Sea (Angeles et al. 2007). The locations of MSDs centered on pentads that fall between June 30 and July 24 (Fig. 4) are shown as hatch-marks on Fig. 6. Note that the temporal convergence of the MSD and maximum pressure anomaly is within the *Transition zone* (Gamble et al. 2007) and overlaps the locally strong and significant power values in Fig. 3. Thus, it appears that the “pressure bump” does not control the timing of the MSD, but may have a role in locally enhancing its strength. This will be discussed further in the next section.

To investigate why the MSD is relatively strong in the western Caribbean, the summertime variability in the climatological surface wind and divergence was examined. Here climatology is used loosely, as the period of QuikSCAT data is from 2000 to 2005. To determine the representativeness of the time period, the wavelet analysis was repeated and a map of maximum power at the 0.320-year period of the wavelet spectrum (as in Fig. 3) was reproduced for GPCP pentad precipitation from 2000 to 2005. A pattern similar to that of the 1979–2005 analysis emerged (not shown), with two of the largest significant power values between Jamaica and the Yucatan peninsula. Thus, the 2000–2005 period appears to be representative of the 1979–2005 climatology. Composites of wind speed and direction and divergence were taken for the early wet season (May 11 to June 14) and mid-summer dry period (June 15 to July 19) for the western Jamaica grid block (Fig. 1a). Vector wind fields are shown

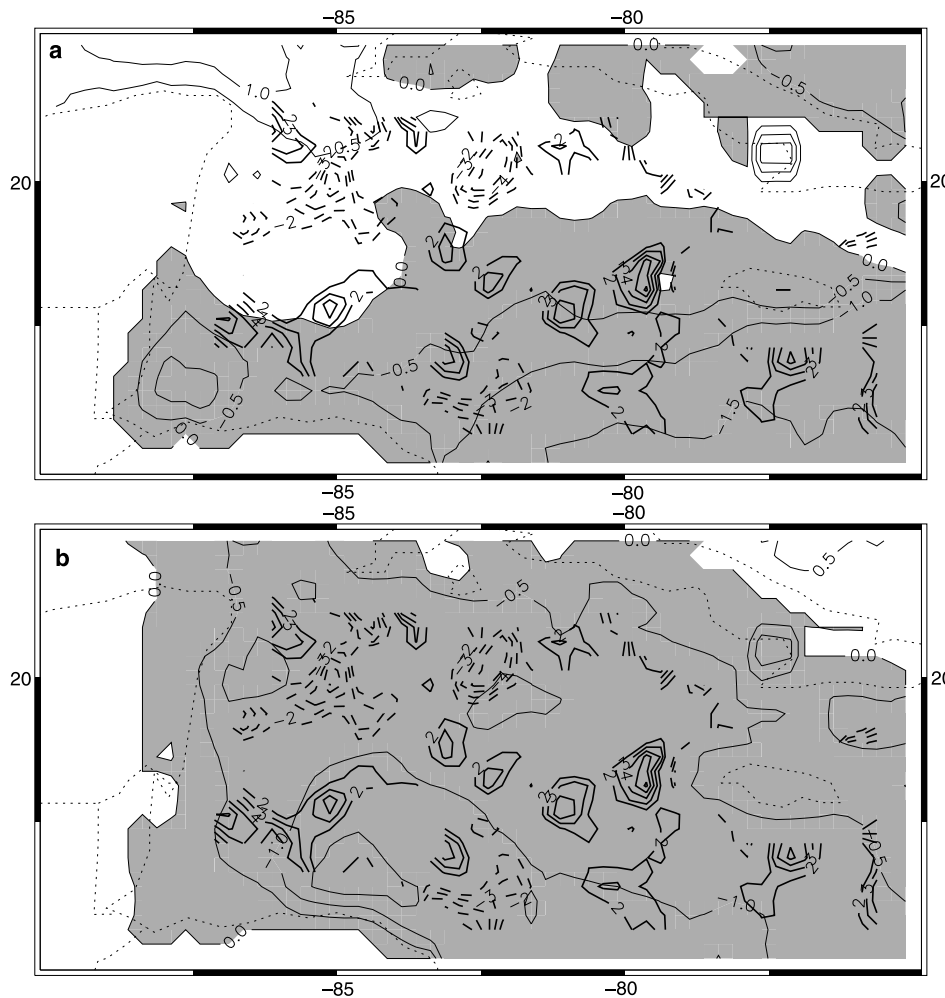


Fig. 8. Wind (m s^{-1}) and divergence ($\times 10^{-6} \text{ s}^{-1}$) differences between the dry period (June 15 to July 19) and the wet period (May 11 to June 14). Divergence differences larger than $+2$ and -2 are shown in both maps with thick solid and dashed contours, respectively. Top (bottom) panel shows zonal (meridional) wind speed differences, with negative values shaded

for May 11 to June 14 in Fig. 7a, and June 15 to July 19 in Fig. 7b. Overall, winds are easterly and stronger in the southern portion of the map. Subtle changes in the wind field from early to mid-summer are presented as the differences in the u-component of wind (Fig. 8a) and v-component of the wind (Fig. 8b). Superimposed on these maps are contours of the difference in divergence between June 15 to July 19 and May 11 to June 14. A 3-grid-block smoothing was applied to all fields. Divergence is inherently noisy because of the spatial differencing, but a band of enhanced divergence during the MSD is evident between Belize and Jamaica, reaching a maximum of $6 \times 10^{-6} \text{ s}^{-1}$. Surface divergence and the accompanying subsidence would be another mechanism, in addition to the “pressure bump” that would strengthen the MSD in the western Caribbean. The enhanced divergence in the western portion of the map appears to be explained by changes in the meridional wind component (Fig. 8b) as the wind vectors are observed to turn southward from May to July near the coast of Honduras (see Fig. 7). On the other hand, the enhanced divergence in the eastern portion of the map appears to be explained by changes in the zonal wind component (Fig. 8a). Generally the easterlies strengthen south of 15° N with the progression of the summer season (see Fig. 7). However, the easterlies have slowed in a small region west of Jamaica near 79° W (Fig. 8a), and this seems to be the cause of the adjacent large divergence differences. Another divergence difference center further to the west near 83° W , also appears to be caused by an east to west gradient of faster winds from May to July. Divergence differences in the center of the map are likely a combination of meridional and zonal wind changes.

4. Discussion and conclusions

The Caribbean experiences a mid-summer drought, which is a significant component of the annual cycle of rainfall. However, we have shown with a wavelet analysis of satellite-based precipitation estimates that the MSD varies both in timing and strength across the Caribbean basin. The MSD first appears in the eastern Caribbean in early-June and can be identified as late as early October in regions of the Gulf of Mexico. These results are consistent with previous stud-

ies of the Caribbean climate that relate the MSD to a westward expansion of the NASH, and a recent paper describing the spatial pattern of the MSD for island weather stations. A new finding in this study is the variation of intensity and significance of the MSD within the Caribbean. The MSD becomes stronger and more significant from east to west, and reaches a maximum in the waters bounded by Jamaica, Cuba, and the Yucatan peninsula.

Several forcing mechanisms may contribute to the observed variability. First, the spatial pattern identified in this study and Gamble et al. (2007) is consistent with an uneven expansion or ridging of the NASH into the Caribbean. Second, the variation in intensity could be related to a localized increase in pressure (“pressure bump”), which occurs in July for most of the Caribbean. However, as discussed above, the MSD expands westward across the basin from May to October. Thus, we propose that when aligned in time with the MSD, the pressure bump serves to strengthen the drought. This combination of NASH expansion and local pressure bump occurs at about the 81.25° longitude. A third mechanism explored here is the changing field of surface wind during the summer months. From May to July, the easterly trades become stronger and turn to the south. This leads to a band of surface divergence from Belize to Jamaica. The surface divergence and subsidence of air would further enhance the MSD in that region. Related to the wind changes, Caribbean island location and orientation may play a role in the localized intensity of the MSD. The fine-scale wind field analysis shows that as the trades strengthen into July, they are impeded by Jamaica, turning and slowing on the leeward side of the island. This creates a very large shift towards divergence in the middle of summer, consistent with the strong and significant MSD.

This study has focused on regional-scale features in the surface climatology, namely an increase in pressure and wind divergence in the central to western Caribbean, that appear to enhance the MSD. To the best of the authors’ knowledge such phenomena have not been identified in previous research. However, one must be mindful that the MSD is forced by synoptic to planetary scale processes. Further, this research has not attempted to assess the potential impacts of intraseasonal (e.g. Madden-Julian Oscillation)

or interannual (e.g. ENSO) climate variability. Curtis (2002) did not identify a relationship between ENSO and the Caribbean MSD, but several other studies (Giannini et al. 2000; Chen and Taylor 2002; Taylor et al. 2002; Ashby et al. 2005) have found links between El Niño, conditions in the Atlantic, and the climate of the Caribbean. Thus, if we are to advance our understanding of the Caribbean MSD, multi-scale studies and modeling experiments are required in order to determine the relative impact of regional-scale climate features identified here with respect to larger-scale forcing mechanisms.

Acknowledgements

The authors would like to thank two anonymous reviewers. This work is funded under NSF award BCS-0718279, “Physical Mechanisms Behind the Mid-Summer Drought”.

References

- Adejuwon JO, Odekunle TO (2006) Variability and the severity of the “little dry season” in southwestern Nigeria. *J Climate* 19: 483–493
- Angeles ME, González JE, Ramirez-Roldán N, Comarazamy DE, Tepley CA (2007) Origins of the Caribbean rainfall bimodal behavior. Proceedings from the 87th American Meteorological Society Annual Meeting, San Antonio, TX: paper 4A.5
- Ashby SA, Taylor MA, Chen AA (2005) Statistical models for predicting rainfall in the Caribbean. *Theor Appl Climatol* 82: 65–80
- Chen AA, Taylor MA (2002) Investigating the link between early season Caribbean rainfall and the El Niño +1 year. *Int J Climatol* 22: 87–106
- Curtis S (2002) Interannual variability of the bimodal distribution of summertime rainfall over Central America and tropical storm activity in the far-eastern Pacific. *Clim Res* 22: 141–146
- Curtis S (2004) Diurnal cycle of rainfall and surface winds and the mid-summer drought of Mexico/Central America. *Clim Res* 27: 1–8
- Gamble DW, Parnell DB, Curtis S (2007) Spatial variability of the Caribbean mid-summer drought and relation to the North Atlantic High. *Int J Climatol* (In press)
- Giannini A, Kushnir Y, Cane MA (2000) Interannual variability of Caribbean rainfall, ENSO, and the Atlantic Ocean. *J Clim* 13: 297–311
- Hastenrath S (1967) Rainfall distribution and regime in Central America. *Arch Met Geophys Biokl, Series B* 15: 201–241
- Hastenrath S (2002) The intertropical convergence Zone of the eastern Pacific revisited. *Int J Climatol* 22: 347–356
- Kalnay E, Kanamitsu M, Kistler R, Collins W and 18 others (1996) The NCEP/NCAR 40-year reanalysis project. *Bull Amer Meteor Soc* 77: 437–471
- Magaña V, Amador JA, Medina S (1999) The midsummer drought over Mexico and Central America. *J Clim* 12: 1577–1588
- Taylor MA, Enfield DB, Chen AA (2002) Influence of the tropical Atlantic versus the tropical Pacific on Caribbean rainfall. *J Geophys Res* 107(C9): 3127, doi:10.1029/2001JC001097
- Torrence C, Compo GP (1998) A practical guide to wavelet analysis. *Bull Amer Meteor Soc* 79: 61–78
- Xie P, Janowiak JE, Arkin PA, Adler R, Gruber A, Ferraro R, Huffman GJ, Curtis S (2003) GPCP pentad precipitation analyses: an experimental data set based on gauge observations and satellite estimates. *J Clim* 16: 2197–2214